Transactions, **SMiRT-26**
Berlin/Potsdam, Germany, July 10-15, 2022
Special session: Impact tests and numerical analyses

PUNCHING FAILURE OF REINFORCED CONCRETE SLABS SUBJECTED TO HARD MISSILE IMPACT, PART I: RECENT TESTS ON INFLUENCE OF SLAB THICKNESS AND SHEAR REINFORCEMENT

Ari Vepsä[1], Christian Heckötter[2], Anthony Darraba[3], Alexis Fedoroff[1], Shohei Sawada[4], Christian Schneeberger[5], Francois Tarallo[6]

[1] Senior Scientist, VTT Technical Research Centre of Finland, Espoo, Finland (Ari.Vepsa@vtt.fi)
[2] Technical Expert, Gesellschaft für Anlagen- und Reaktorsicherheit (GRS) gGmbH, Cologne, Germany
[3] Structural Engineer, Électricité de France (EDF), Lyon, France
[4] Group Leader, Kajima Corporation, Tokyo, Japan
[5] Deputy Section Head, Swiss Federal Nuclear Safety Inspectorate ENSI, Brugg, Switzerland
[6] Civil Engineer - Senior Expert, Institut de Radioprotection et de Sûreté Nucléaire IRSN, Fontenay- aux-Roses, France

ABSTRACT

A series of seven hard impact tests were carried out with 300 – 350 mm thick reinforced concrete slabs. The goal of the study was to verify the results obtained in earlier tests with 250 mm thick slabs. The results show that the effect of shear reinforcement on the punching resistance of the slabs increases when the slab thickness increases. The results also indicate that concrete parameters other than the compressive strength can affect the behaviour of the slabs considerably. More research is needed to verify and quantify the results more accurately.

INTRODUCTION

Impact of a hard or semi-hard projectile, like an aircraft engine, is one possible threat for the safe operation of nuclear power plants. Testing of reinforced concrete (rc) structures against different types of impact loading has been carried out at VTT in jointly funded international projects called IMPACT since 2005. Hard impact testing has been an essential part of these campaigns. Test parameters of this series included impact velocity, shear- and bending reinforcement ratio and concrete strength, among others. Different failure modes including penetration, scabbing, spalling and perforation occurred in this series. One shortcoming of this test matrix was the limitation to one single slab thickness of 250 mm. Therefore, a recent test series is dealing with a variation of slab thickness. In this context, one test with a slab thickness of 300 mm and six tests with a slab thickness of 350 mm have been carried out so far. The tests with a slab thickness of 350 mm addressed the effect of shear reinforcement on slab damage and punching resistance. One goal of the tests was to verify for thicker slabs and smaller ratios of projectile diameter to slab thickness earlier results with 250 mm thick rc slabs described for instance by Orbovic et al. (2015).

METHODS

A series of seven hard impact tests were carried out with 300 mm and 350 mm thick rc slabs. The tests were carried out within NEREID project with VTT test apparatus described in the work by Lastunen et al. (2007). Six tests from previous projects are included in the study for comparison. The test matrix is presented in

Table 1. The table includes information regarding the slab thickness, H, impact velocity, v_0, projectile mass, m_p, concrete unconfined compression strength, f_c and splitting tensile strength, f_{ct}. The expected ballistic limit for tests 1-7, $v_{P,Exp.}$, was predicted before the tests based on the results from the earlier tests and the effect of variable parameters on the punching resistance of the slabs according to selection of semi-empirical formulas.

Table 1: Test matrix.

Test	Test id	Notes	H	Shear reinf.	v_0	Projectile version	m_p	f_c	f_{ct}	$v_{P,Exp.}$
			mm		m/s		kg	MPa	MPa	m/s
1	[a)]IRIS P1	*	250	-	136	H0	47.38	60	4.04	
2	[a)]IRIS P2	*	250	-	135	H0	47.46	57.4	3.34	
3	[a)]IRIS P3	*	250	-	137	H0	47.32	58.3	3.34	
4	AT2	*	250	D12T	140	H0	47.1	57.0	3.90	
5	A12	*	250	-	110	H0	47.44	50.4	3.17	
6	P6	*	250	D10T	111	H1	47.46	49.7	3.51	
7	ITP1		300	-	138	H2	47.4	59	4.10	125-130
8	ITP2		350	-	149	H2	47.9	60.5	3.97	134-146
9	ITP2R		350	-	162	H3	47.63	64.5	4.78	137-149
10	ITP2RR		350	-	144	H3	47.5	47.5	3.97	127-134
11	ITP4		350	D12T	152	H2	48.0	61.0	3.98	155-171
12	ITP4R		350	D12T	144	H3	47.4	63.6	4.78	157-173
13	ITP4RR		350	D12T	156	H3	47.34	47.5	3.97	146-155
*Comparison test from another project										
[a)] IRIS_2010 tests, (Vepsä et al., 2011)										

The tested slabs were simply supported in both directions with in-plane dimensions of 2.1 * 2.1 m and the span width being 2.0 m in both directions. The slabs were reinforced with D10 mm B500B rebars with spacing of 90 mm in both directions and on both faces with the concrete cover being 20 mm. Shear reinforcement, when used, was realized in a form of D10 or D12 mm T-headed bars (D10T, D12T) with spacing of 90 mm in both directions. A drawing of the reinforcement used in test ITP4 is shown in Figure 1 which presents one quarter of a symmetric slab.

The projectiles used in the tests had a solid steel dome at the front, followed by a steel pipe filled with lightweight concrete. An aluminium tail is attached to the rear of the projectile so that its residual velocity after perforation could be deduced using high shutter speed video footage. The projectile has been modified and strengthened along the years when need has arisen. Four versions of the projectile have been used. The projectile is show in Figure 2 together with the main differences between the versions. The main information regarding the different projectile versions is collected in Table 2. This information includes the outer diameter, D_o, the body wall thickness, t_b, the length (excluding tail), L, the radius of the front dome, r_d, and the target mass of the projectile, $M_{M;}$.

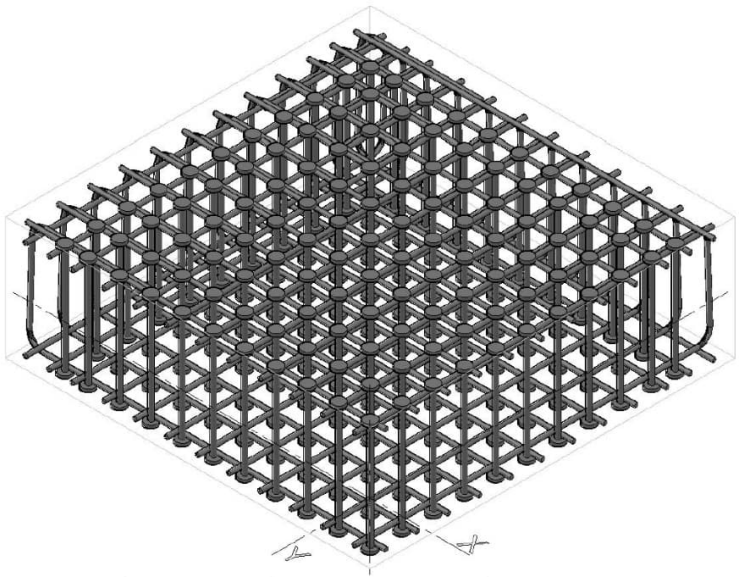

Figure 1. Schematic drawing of the reinforcement used in the test with T-headed bars. Quartile of the slab is shown.

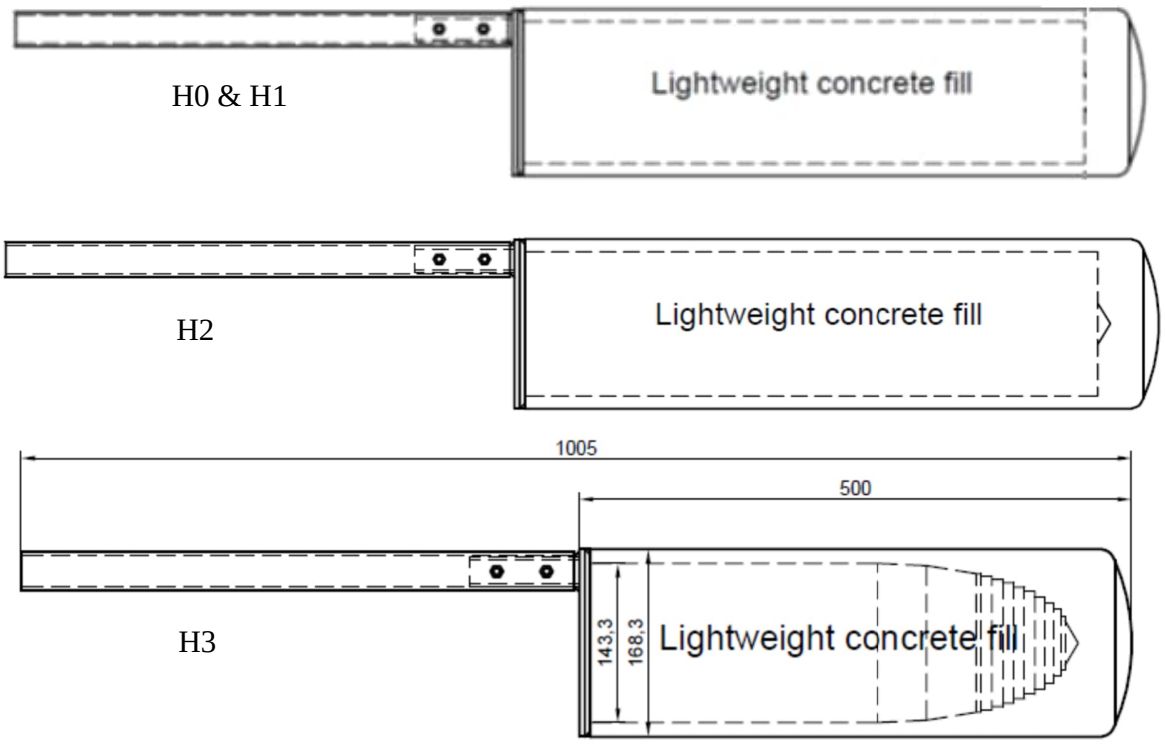

Figure 2. The projectile types H0 – H3 used in the tests.

Table 2: Main parameters of the different projectile versions.

Projectile version	Steel grade	D_o	t_b	L	r_d	M_M	Body type
		mm	mm	mm	mm	kg	
H0	S355 J2H	168.3	10	640	187	47.5	Welded dome & pipe
H1	S355 J2H	168.3	12.5	640	187	47.5	Welded dome & pipe
H2	S355 J2H	168.3	12.5	640	187	47.5	Cut from one piece
H3	S355 J2H	168.3	12.5	500	187	47.5	One-piece, gradually thickening wall

The tests were documented with two high speed cameras. The footage from the cameras was used to determine the residual velocity, V_R, of the projectile in case it perforates the slab. The ballistic limit for the target slab can be computed backwards using the energy balance of the impact:

$$E_{k0} = E_P + E_M + E_G + E_R, \quad (1)$$

where E_{k0} is the kinetic energy of projectile at the moment of the impact, E_P is the critical initial kinetic energy of the projectile required to just perforate the target, E_M is the energy dissipated by the projectile deformation, E_G is the energy associated with global effects of the impact and E_R is the residual kinetic energy of the projectile and the concrete plug that is detached from the surrounding medium. A common assumption is

$$E_R = \frac{(M_M + M_c)V_R^2}{2}, \quad (2)$$

where M_c is the mass of the detached concrete plug.

The effect of different factors on the punching resistance of rc walls can be estimated by studying the existing empirical and semi-empirical formulas which have been developed during the years for calculation of penetration depth of a hard projectile. A good summary of these can be found for example in the work by Li et al. (2005). In general, these formulas give the slab thickness required to prevent perforation, e, as a function of projectile and target related parameters. Due to the expensive nature of the tests which these formulas are based on, complex behavior of the target response has had to be reduced to very limited set of parameters which effect could be studied to sufficient extent. The most used of these are the projectile related parameters of mass, diameter, impact velocity and the nose shape as well as target related parameter of concrete compressive strength. Other used parameters that come into question include the amount and spacing of longitudinal reinforcement as well as density, Young's modulus and maximum aggregate size of concrete. Less studied parameters include pre-stressing of concrete as well as the amount and the type of shear reinforcement.

While it's not the purpose of this paper to study in depth the experimental perforation formulas or the effect of all different factors on the punching resistance, it is justified to pay attention to the parameters of interest in the current study. These are the slab thickness or impact velocity, concrete strength and shear reinforcement. In many formulas the slab thickness required to prevent perforation, e, is considered to depend on the compressive strength of concrete as follows $e \propto f_c^{0.5}$. However, dimensional analysis of the formulas suggests exponent to be 1.0. Similar relationship between e and the impact velocity V_0 is $e \propto V_0^{1.33} \ldots V_0^{2.0}$. Shear reinforcement is generally not taken explicitly into account in the formulas.

The concrete batches for slabs 1 – 6 were subjected to limited set of basic mechanical material tests that included unconfined compression strength, f_c, splitting tensile strength, f_{ct}, and Young's (secant) modulus, E_c. The values of f_c and f_{ct} are included in Table 1. The concrete batches used for slabs 7 - 13 were

subjected to more versatile testing. This was justified by gradually increased recognition of concrete's material properties' importance in the punching resistance followed by a desire to understand more thoroughly it's behaviour under impact loading as well as need for more comprehensive set of parameter values to be used in numerical modelling. The results of these extensive material tests are collected in Table 3.

Table 3: Concrete material test results for batches used to cast slabs 7-13.

Test	Standard	Quantity	ITP*	ITP…R	ITP…RR	Unit
T1.1	SFS-EN 12390-3	Max. Stress (Force driven)	60.2	64.5	47.5	MPa
		Strain at max. force	-	0.38	0.37	%
T1.2	SFS-EN 12390-3	Max. Stress (Displacement driven)	57.2	60.7	45.3	MPa
		Strain at max. force	0.29	0.31	0.36	%
		Strain at failure (0.1 f_c)	0.62	0.72	0.95	%
		Fracture energy in compression	-	-	13036	N/m
T2	SFS-EN 12390-13	Secant modulus	34.131	31.498	31.645	GPa
		Poisson's ratio	-	0.211	0.198	-
T3.1	SFS-EN 14652 + A1	Fracture energy	100.1**	142	103	N/m
		Tensile strength	3.2	3.08	2.77	MPa
T4.1	Own method	Triaxial comp. Strength (Confinement ratio 50%)	117	116.7	101.2	MPa
		Axial strain at max.	1.90	0.99	2.43	%
		Lateral strain at max.	-0.28	-0.14	-0.37	%
T4.2	Own method	Triaxial comp. Strength (Confinement ratio 100%)	164	141	165.4	MPa
		Axial strain at max.	2.7	1.4	3.96	%
		Lateral strain at max.	-0.2	-0.21	-0.45	%
T5	SFS-EN 12390-6	Splitting tensile strength	4.04	4.78	3.97	MPa

*The results in the table are the average values across the individual slabs ITP1, 2 & 4, tested at the same time than the slabs themselves.

** Measured using slightly different method than the values for R and RR tests.

RESULTS

Still frames extracted from high shutter speed video footage taken during test ITP4RR are shown in Figure 3 and 4. The frames have been taken at the moment of the impact and then 2.5, 5.0 and 7.5 ms after that. The black and white stripes on the flank of the projectile are each 100 thick.

Figure 3. Top view photos of the impact ITP4RR at the moment of the impact and 2.5, 5.0 and 7.5 ms after that.

Figure 4. Side-view photos of the impact ITP4RR at the moment of the impact and 2.5, 5.0 and 7.5 ms after that.

Test ITP1, ITP2 and ITP4 resulted undesired fracturing failure of the projectiles, making them less hard than what was intended. The energy dissipated by the fracturing of the projectile was estimated by measuring the fractured area and assuming relatively low literature based critical plain strain stress intensity factor of K_I = 37.5 Mpa/√m for the projectile material. The true value of E_M can vary a lot from this as the value of K_I can change greatly between different heats of the same material. In addition to fracturing, the front part of the projectile underwent serious deformation. Damages of the projectile used in test ITP4 are visible in the photograph at the top row in Figure 5. The strengthened projectile used in test ITP4R is shown for comparison at the bottom of the figure.

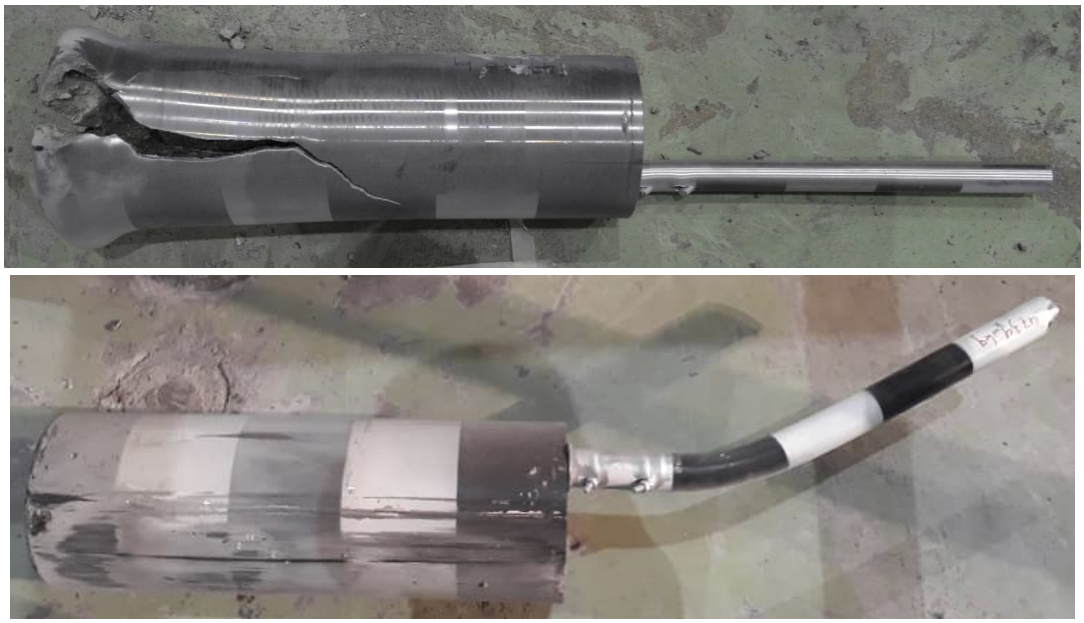

Figure 5. The projectiles used in test ITP4 (top) and ITP4R (bottom) after the test.

The main results of the tests have been compiled in Table 4. The results include the residual velocity, $v_{Res.}$, in case of perforation, the penetration depth, x, in case of no perforation, the mass of detached concrete, m_{dc}, the amount of it retained within the reinforcement (if known), $m_{dc,R}$, the area of scabbed concrete at the rear surface, $A_{sc.}$, the area of spalled concrete at the front surface, $A_{Sp.}$, and the additional areas of cracked concrete, $A_{Cr.}$, at the rear and front surfaces. The table also includes the fractured area of the projectile, $A_{frac.}$, in tests ITP1, ITP2 and ITP4 together with the resulting energy dissipated in the fracture process.

Table 4: The main test results.

Test	v_0	v_{Res}	x	m_{dc}	Notes	$m_{dc,r}$	$A_{Sc.}$	$A_{Cr.}$	$A_{Sp.}$	$A_{Cr.}$	$A_{frac.}$	E_m
	m/s	m/s	mm	kg		kg	m^2	m^2	m^2	m^2	mm^2	kJ
IRIS P1	135.9	34		101	*		1.06	-	0.11			
IRIS P2	134.9	45		116	*		1.10	-	0.10			
IRIS P3	136.5	36		121	*		1.12	0.18	0.10			
AT2	140	45		24	**		0.23	0.02	0.09			
A12	110	21		108	**		0.97	0.53	0.23			
P6	111	5		35	**		0.34	0.07	0.10			
ITP1	138	25		180		48	1.18	0.27	0.25		20628	138
ITP2	149	-	X	220		78	1.29	0.51	0.30	0.11	29379	197
ITP2R	162	48		214		85	1.08	0.38			39381	264
ITP2RR	144	35		210		110	1.32	0.44	0.29	0.20		
ITP4	152	-	37	28			0.35	0.02	0.20			
ITP4R	144	-	150	50	**		0.45	0.04	0.16	0.02		
ITP4RR	162	29		44			0.34	0.08	0.19			
* Estimated from the measured crater depth.												
** Estimated from the known A_{SC}- m_{dc} relationship from previous tests.												
X Penetration depth could not be measured. Concrete completely crushed. Close to perforation.												

Because of the impacts, concrete scabbed off from both from the front and the back surfaces of the tested slabs. This is caused by the impact induced compression wave changing sign and transforming to a tensile one when reflecting at the rear surface of the slab. As an example, front and rear surfaces of slabs ITP2RR and ITP4RR are shown in Figures 6 and 7. As can be seen, inclusion of T-headed bars reduced the amount of concrete scabbed off at the rear surface significantly.

Vertical cross-sections of quartiles of selected slabs are shown in Figure 8. The slabs are presented in pairs with the ones without shear reinforcement are presented on the left and those with it on the right. Shear reinforcement strengthens the slab against tensile loads reducing shear cone formation. As can be seen from the cross-section of test ITP 4, numerous cracks can be observed around the impact area. Alignment of these cracks change from vertical at the centre of the slab to higher than 45 ° angle further away from it. Similar cracking can be observed also in the other slabs with shear reinforcement. Despite of these cracks, none of the shear reinforced slabs with perforation demonstrated a large shear cone formation like the perforated slabs without shear reinforcement. Instead, a narrow shear plug with almost uniform diameter was formed by the impacting projectile and separated from the surrounding medium. Shear cone formation can be found only near the rear surface of the shear reinforced slabs when the spacing of the shear reinforcement is too sparse to prevent it to happen. Changing the shape of the detached concrete from a cone to cylinder also reduced the amount of it. This means that once the ballistic limit of a slab is exceeded, the residual velocity increases faster in tests with shear reinforcement than in those without it.

Figure 6. Front surface of slabs ITP2RR (left) and ITP4RR (right) after the test.

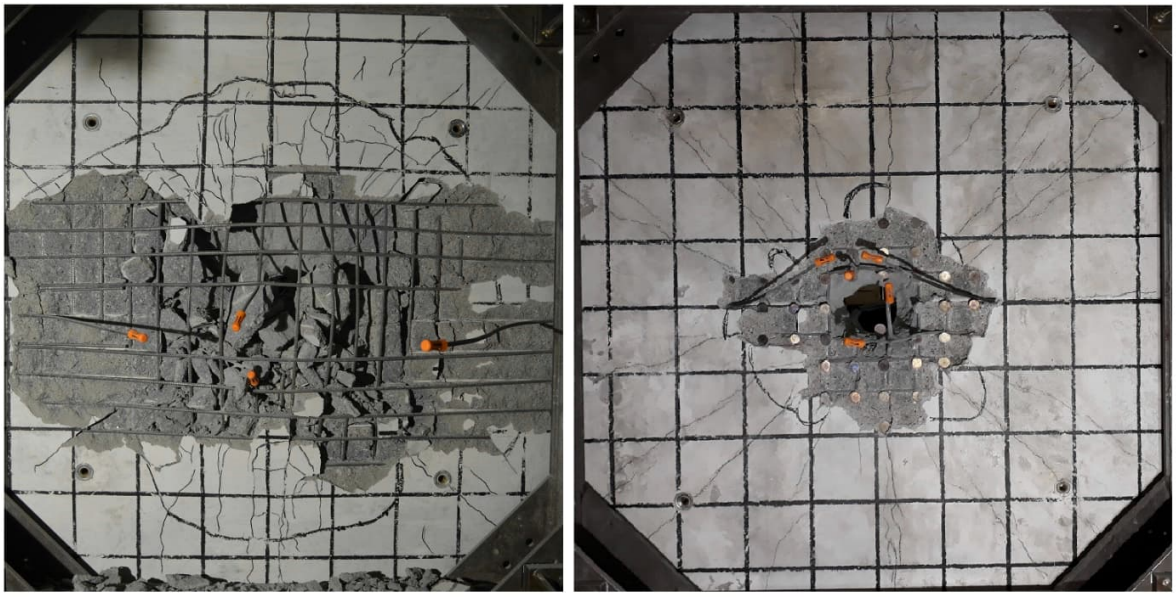

Figure 7. Rear surface of slabs ITP2RR (left) and ITP4RR (right) after the test.

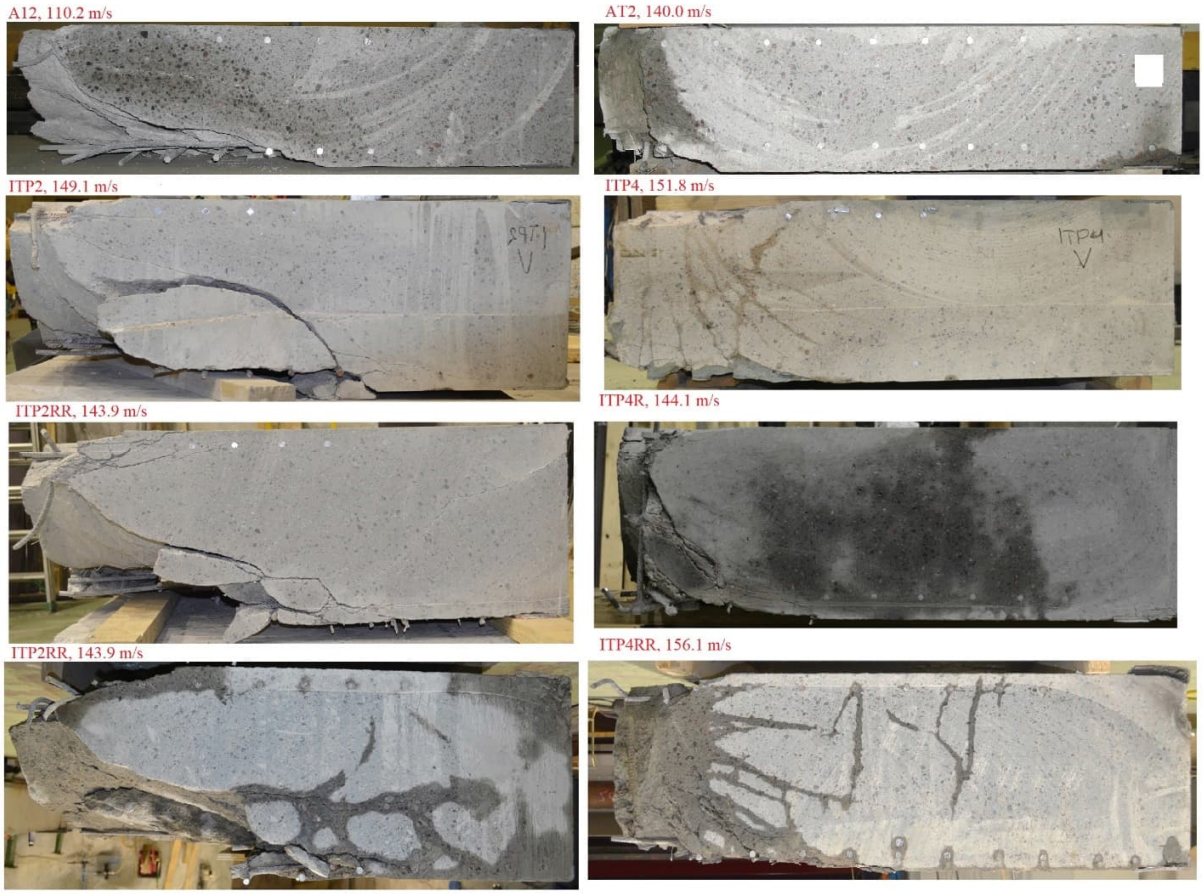

Figure 8. Vertical cross-sections of the sawn quarters of the slabs.

The kinetic energy required for perforation, E_P, in the studied tests is presented in Figure 9 as a function of concrete compressive strength. E_P is presented relative to the unit target thickness. The squares represent tests with shear reinforcement and the dots without it. 250 mm thick slabs are presented with black and red, 300 mm thick with green and 350 mm thick with blue color. Only the tests resulting perforation have been included. It should be noted how scattered the results obtained with the thicker slabs (ITP) are compared to the test with 250 mm slabs. It is also worth noting that E_P increases 62 % when the shear reinforcement is introduced to 350 mm thick slab (ITP2RR vs ITP4RR). In 250 mm thick slabs this can be around 20 - 30 % as exemplified by the difference between AT2 (with T-headed bars) and IRIS-tests. This indicates increasing importance of the T-headed bars with increasing slab thickness. It can also be seen how the effect of the T-headed bars is reduced when the bar diameter is reduced to 10 mm (P6 vs A12) although variance in the results may well explain part of this reduction. The least squares straight line has been fitted into the figure for 250 mm thick slabs without shear reinforcement.

Due to smaller amount of global damage as well as detached concrete, the ballistic limit computed for the slabs with shear reinforcement can be considered as more accurate than those computed for the slabs without shear reinforcement. This is because the ballistic limit is usually computed assuming that the energy dissipated in global damage is negligible and that the residual velocity of the detached concrete is the same than that of the projectile. Both assumptions are quite crude, and their effect is emphasized in tests without shear reinforcement.

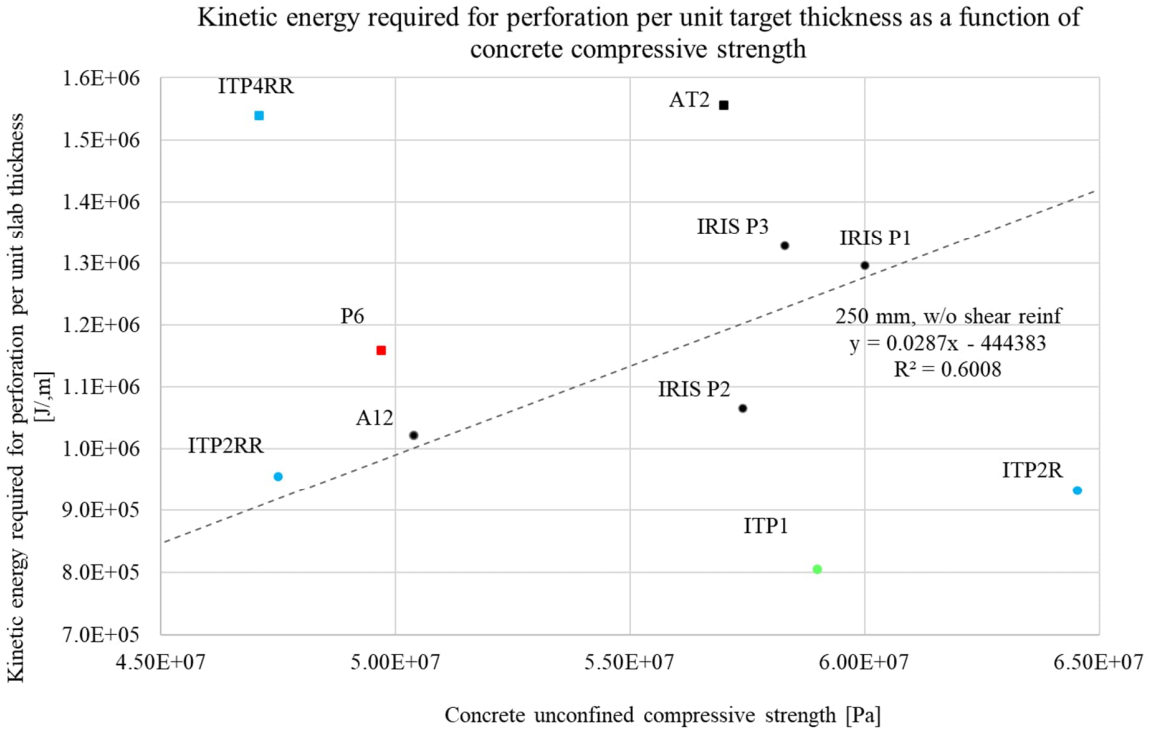

Figure 9. Kinetic energy required for perforation per unit target thickness as a function of concrete compressive strength.

CONCLUSIONS AND DISCUSSION

The effect of the shear reinforcement on the punching resistance seems to increase when the slab thickness increases. Relative amount of detached concrete seems to decrease slightly compared to 250 mm thick slabs. The punching resistance of slab ITP2R was surprisingly low when compared with ITP2RR. One explanation for this can be that concrete parameters other than f_c affect the punching resistance of the slabs considerably. For example, the strains measured at maximum strength in triaxial tests were much lower for slab ITP2R than for ITP2RR. In general, more research is required to validate and quantify the results.

REFERENCES

Lastunen, A., Hakola, I., Järvinen, E., Hyvärinen, J. and Calonius, K. (2007). ”Impact test facility,” *Proceedings of SMiRT-19*, Toronto, Canada, 2007, Paper id. J08/2-1.

Li Q.M., Reid S.R., Wen H.M., Telford A.R. (2005). “Local impact effects of hard projectiles on concrete targets,” *International Journal of Impact Engineering*, 2005, 32, 224-284.

Orbovic, N., Sagals, G. and Blahoianu, A. (2015). “Influence of transverse reinforcement on penetration resistance of reinforced concrete slabs under hard missile impacts”. *Nuclear Engineering and Design*. 295. 716-729. http://dx.doi.org/10.1016/j.nucengdes.2015.06.007.

Vepsä, A., Saarenheimo, A., Tarallo, F., Rambach, J.-M., Orbovic, N. (2011). “IRIS_2010 –Part II: Experimental Data,” *Transactions of SMiRT 21*, New Delhi, India, 2011, paper 520.